Unconventional access to a solvatochromic nickel (II) dye featuring a coordination-induced spin crossover behavior

Zhongrui Chen, Khrouz Lhoussain, Christophe Bucher, Denis Jacquemin, Dominique Luneau, Olivier Siri

Unconventional access to a solvatochromic nickel (II) dye featuring a coordination-induced spin crossover behavior

Zhongrui Chen,[a] Khrouz Lhoussain,[b] Christophe Bucher,[b] Denis Jacquemin,[c]* Dominique Luneau,[d] and Olivier Siri[a,*]

a Aix Marseille Université, CNRS UMR 7325 Centre Interdisciplinaire de Nanosciences de Marseille (CINaM), Campus de Luminy 13288 Marseille cedex 09, France. Email: olivier.siri@univ-amu.fr

b ENS de Lyon, CNRS UMR 5182, Université Claude Bernard Lyon 1, Laboratoire de Chimie, 69342, Lyon, France

c Université of Nantes, CNRS, CEISAM, UMR 6230, Nantes, France.
Email: Denis.Jacquemin@univ-nantes.fr

d Laboratoire des Multimatériaux et Interfaces, UMR 5615, Université Claude Bernard Lyon 1 -F-69622 Villeurbanne cedex, France.

ABSTRACT

We report the synthesis of a square-planar nickel complex in which the metal center is located in a NOON environment. Promoting its axial ligation triggers a spin state switching process which is accompanied by a change of the absorption properties depending on the solvent. Indeed, a strong solvatochromic shifts could be observed in the presence of DMSO or pyridine, highlighting the key interplay between the donor strength of the solvent and the optical properties of the complex. The optical and magnetic properties of this compound in coordinating media have been carefully investigated through combined experimental/theoretical approaches.

Keywords: Ni complex, solvatochromism, magnetism, quinone

1 INTRODUCTION

Quinoidal ligands have recently attracted considerable attention due to their remarkable ability to form complexes displaying specific redox and optical properties [1]. They include the 2,5-diamino-1,4-benzoquinonediimines (QDIs, **1**) whose very first member (azophenine, R = Ph) was reported as early as 1875, by self-condensation of aniline [2]. Various *N*-alkylated analogues have been reported more recently [3] together with numerous dinuclear complexes isolated from **1**, which have proved useful in a wide spectrum of applications, ranging from catalysis and magnetism to electrochromism and electronics [4].

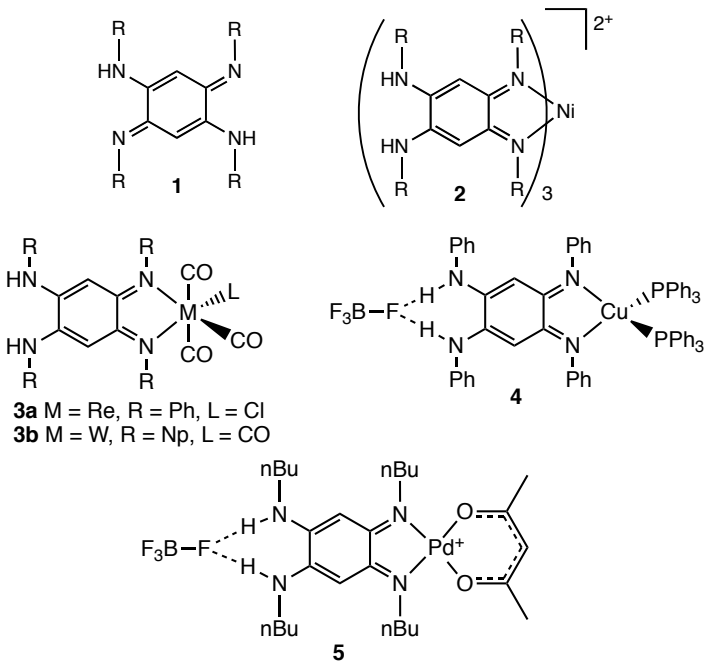

3a M = Re, R = Ph, L = Cl
3b M = W, R = Np, L = CO

In contrast, only five mononuclear QDI complexes have been reported so far wherein the metal centre is found in different environments: octahedral with M = Ni(II) [5] (**2**), Re(I) [6] (**3a**) and W(0) [7] (**3b**), tetrahedral with M = Cu(I) (**4**) [8] and square-planar with M = Pd(II) (**5**) [9]. As illustrated on the complexes above, those compounds are stabilized in all cases by a rearrangement of the ligand (a metal-induced *para* $\rightarrow$ *ortho* tautomerism). Different electronic properties could be observed depending on the metal centre and its environment [4]. For instance, UV–Vis absorptions of the copper (**4**) and tungsten (**3a**) complexes shows a broad absorption band at 525 and 620 nm, respectively, attributed to MLCT transitions. This striking feature comes from the low-lying π^* orbitals of type **1** quinoidal ligands which can mix extensively with the valence *d*-orbitals of the metal, giving complexes wherein the electrons are delocalized over both the metal and the ligand (the so-called π-d conjugation) [10].

Surprisingly, the impact of the spin state of the metal on the electronic properties of QDI complexes has never been studied whereas its control has attracted much interest over the past decades. Particular attention focused on Ni(II) complexes whose spin states [low spin (LS) *S* = 0 ; and high spin (HS) S = 1] can be switched upon controlling the coordination number and geometry of the metal center [11]. As illustrated in Fig. 1, promoting axial ligation onto square-planar nickel centres is a well-known strategy to trigger a spin state switching process, the formation of pentacoordinated (square-pyramidal) or hexacoordinated (octahedral) complexes being accompanied by a change of the spin state of the nickel(II) centre from *S* = 0 to *S* = 1.

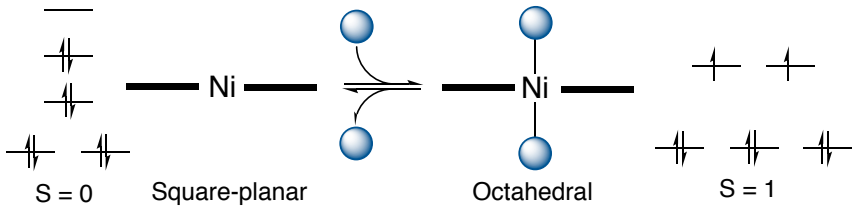

Figure 1 Qualitative representation of the spin states of Ni(II) in square planar and octahedral environments.

In this context, a number of Ni(II) complexes showing solvatochromic behaviour have been synthesized previously and their spectroscopic properties have been analysed in terms of geometrical parameters involving changes in the coordination sphere [11-12]. However, recent studies have also established that solvent molecules do not coordinate to nickel centres complexed by strong-field ligands providing NOON environments [13].

Herein, we report the synthesis of a new square-planar mononuclear nickel complex **7** based on **1**, in which the metal center is located in a NOON environment. This complex was found to exhibit a coordination induced change of spin state associated to strong solvatochromic shifts observed in the presence of DMSO or pyridine, highlighting the key interplay between the donor strength of the solvent and the optical properties of the complex. The optical and magnetic properties of this compound in coordinating media have been carefully investigated through combined experimental/theoretical approaches.

2. EXPERIMENTAL SECTION

Synthesis of 7

Route A: To a solution of ligand **2** (R = nBu) (m = 25 mg, 69.3 µmol, 1 equiv.) in 1,4-dioxane (v = 5 mL), Ni(acac)2 (m = 17.8 mg, 69.3 µmol, 1 equiv.) and HBF4 aq. (0.153 M, v = 453 µL, 69.3 µmol, 1 equiv.) were added. The mixture was stirred overnight. Then the solvent was removed under

reduced pressure. The resulting solid was taken by Et_2O (v = 30 mL), filtrated, washed with Et_2O (v = 2 x 30 mL) and dried under vacuum to afford the desired product **7** as a dark red powder (m = 34 mg, 56.2 µmol, 81% yield).

^{1}H NMR (400 MHz, $CDCl_3$ 294 K): δ(ppm) = 6.88 (br t, 2H, N*H*), 5.54 (s, 1H, C*H*-acac), 5.09 (s, 2H, N-C-C-*H*), 3.18 (dt, $^3J_{HH}$ = 5.6 Hz, $^3J_{HH}$ = 7.2 Hz, 4H, NH-CH_2-), 2.68 (t, $^3J_{HH}$ = 7.5 Hz, 4H, N-CH_2-), 1.95 (s, 6H, CH_3-acac), 1.75-1.68 (quintet, $^3J_{HH}$ = 7.5 Hz, 4H, NH-CH_2-CH_2-), 1.55-1.45 (m, 4H, N-CH_2-CH_2-), 1.45-1.34 (m, 8H, -CH_2-CH_3), 0.98-0.93 (m, 12H, -CH_2-CH_3). ^{13}C NMR (100 MHz, $CDCl_3$, 294 K): δ(ppm) = 187.2, 164.9, 148.8, 102.1, 86.8, 45.4, 44.1, 31.6, 29.1, 25.5, 20.7, 20.3, 14.0, 13.7. ^{19}F NMR (376 MHz, $CDCl_3$, 294 K): δ(ppm) = -150.60, -150.67. HRMS (ESI-TOF): m/z $[M]^+$ for $C_{27}H_{47}N_4O_2Ni^+$ calcd. 517.3047, found 517.3044, err. < 1 ppm. Elemental analysis for $C_{27}H_{47}BF_4N_4NiO_2$•1/6Et_2O: calcd. C 53.81, H 7.94, N 9.07; found C 54.07, H 7.71, N 9.19.

Route B: In a flask, $Ni(acac)_2$ (m = 51.4 mg, 200 µmol, 1 equiv.) and $NaBF_4$ (m = 22 mg, 200 µmol, 1 equiv.) were dissolved in a diluted HCl aq. solution (v = 66 µL 12N HCl in v = 1 mL water dist., 796 µmol, 4 equiv.). Then a solution of ligand **2** (R = nBu) (m = 72 mg, 200 µmol, 1 equiv.) in 1,4-dioxane (v = 10 mL) and NaHCO3 (m = 80 mg, 952 µmol, 4.8 equiv.) were added. The dark blue mixture was stirred overnight. Then the solvent was removed under reduced pressure. The residue was purified by column chromatography (silica 60F, DCM/MeOH, 95/5). After evaporation, the resulting solid was washed with Et_2O, filtrated and dried under vacuum to afford **7** as a dark red powder (m = 90 mg, 149 µmol, 75% yield).

Route C: To a solution of 6a (m = 30 mg, 44.5 µmol, 1 equiv.) in 1,4-dioxane (v = 6 mL), HBF4 aq. (0.153 M, v = 596 µL, 91.2 µmol, 2.05 equiv.) was added. The mixture was stirred overnight. Then the solvent was removed under reduced pressure. The resulting solid was taken up in DCM (v = 1 mL), precipitated with Et2O (v = 30 mL), filtrated, washed with Et2O (v = 3 x 30 mL) and dried under vacuum to afford 8a as a dark red powder (m = 23 mg, 38.0 µmol, 86% yield).

3. RESULTS AND DISCUSSION

3.1 Synthesis

The mononuclear Ni(II) complex **7** has been prepared employing a known strategy proceeding through metalation of ligand **6** with $Ni(acac)_2$ in the presence of acid (HBF_4) (Scheme 1) [9]. Alternatively, we have developed another route involving the dinuclear complex **8** and HBF_4 as key reactants. In this synthetic route, the protonation of **8** undergoes the demetallation of one metal center and the stabilization of the corresponding mononuclear compound **7** by tautomerism rearrangement.

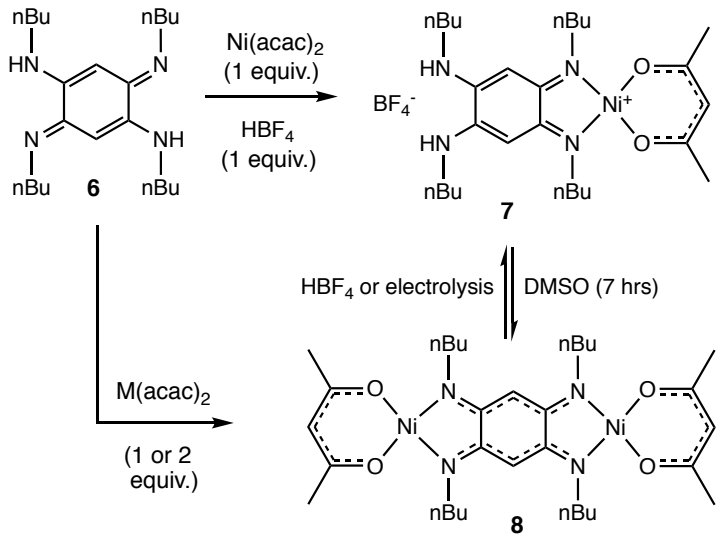

Scheme 1 Synthesis of the mononuclear Ni(II) complex **7**.

We also found that the mononuclear complex **7** can be readily obtained using electrochemical methods, upon submitting the binuclear analogue **8** to a potentiostatic electrolysis experiment. Early evidences revealing the existence of chemical steps (C) coupled to the oxidation (E) of **8** have been provided by cyclic voltammetry measurements showing that both oxidation waves observed in the accessible potential range (Fig. 2A) remain fully irreversible at all investigated scan rates (50mV/s to 20 V/s). This assumption was further supported by the observation of additional waves on the reverse scan (indicated with stars in Fig. 2A) attributed to the reduction of different EC products generated *in-situ* at the electrode interface upon oxidation of **8**. The univocal nature of the chemical step coupled to the first oxidation of **8** occurring at $E_p \approx 0.1$ V was however initially suggested by the observation of a single reduction wave centred at $E_p = -0.5$ V (* in Fig. 2A). *In-situ* spectroelectrochemical (SEC) analyses have then been carried out to obtain further insights into the nature of the electrogenerated species. The EC process has been investigated at a preparative scale upon carrying out a potentiostatic coulometry experiments in a three-compartments electrochemical cell using a platinum plate as a working electrode whose potential was held at E_{ap} =0.4V. The advancement of the electrolysis was followed by steady state voltammetry measurements carried out at a rotating disk electrode. As can be seen in the curves depicted in Fig. 3B, the one electron oxidation of **8** yields a stable EC product, getting oxidized above 0.6 V and reduced at about $E = -0.5$ V (dashed curves in Figure 3B), which is in agreement with by the CV data discussed above (* in Fig. 2A).

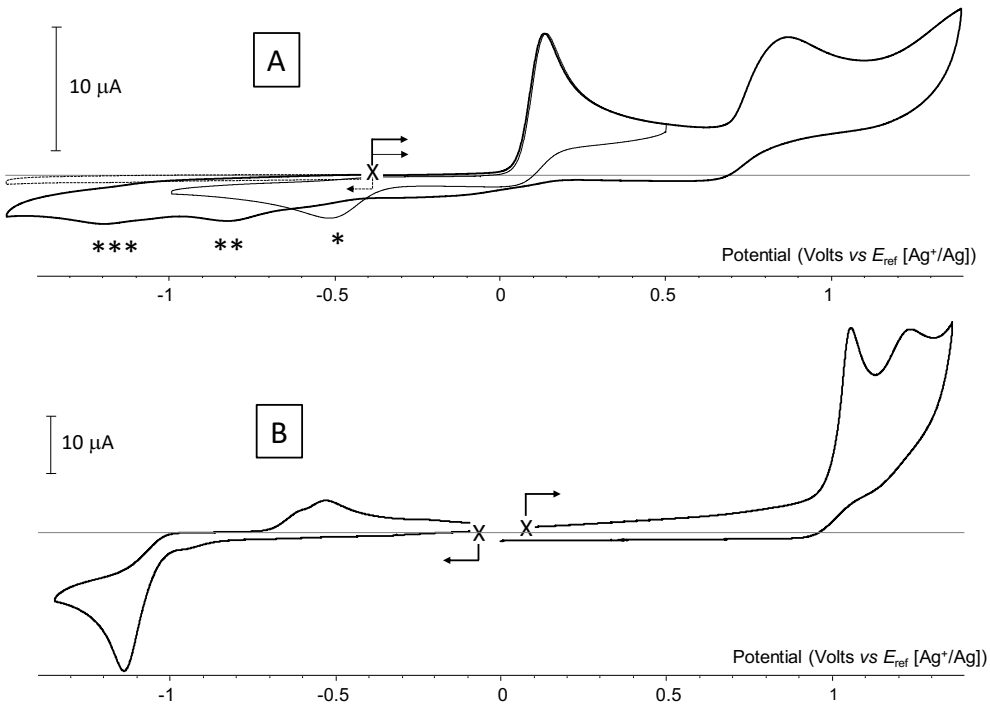

Figure 2 A) Voltammetric curves of a dichloroethane ($TPABF_4$ 0.1 M) solution of **8** (1×10^{-3} M) recorded at (solid line) a stationary carbon working electrode (Ø = 3 mm, v = 0.1 $V \cdot s^{-1}$) (B) Voltammetric curves of a dichloromethane ($TPABF_4$ 0.1 M) solution of **7**(BF_4) recorded at a stationary vitreous carbon working electrode (Ø = 3 mm, v = 0.1 $V \cdot s^{-1}$).

Then, we found that the solution obtained after completion of the bulk oxidation is ESR silent (Q band, 77 K), which provides support for an oxidation centred on the ligand rather than on the metal followed by a rapid conversion into a diamagnetic product. The electrolysis is moreover accompanied by colour changes which are revealed in Fig. 3A by the development of new absorption bands centred at 350 nm and 640 nm. Work-up of the electrolyzed solution involved evaporating the reaction mixture to dryness under reduced pressure, adding water and filtering the solid material to afford a crude product which was purified by flash chromatography. TLC analysis of the latter material revealed one major component which could be identified as being the mono nickel complex **7** (see below). The CV curves shown in Fig. 2A and 2B bring to light a few key differences between the electrochemical signatures of **7** and **8**. Unlike **8**, **7** can be reduced in the accessible potential range and its oxidation wave is shifted toward more positive potential values by more than 900 mV.

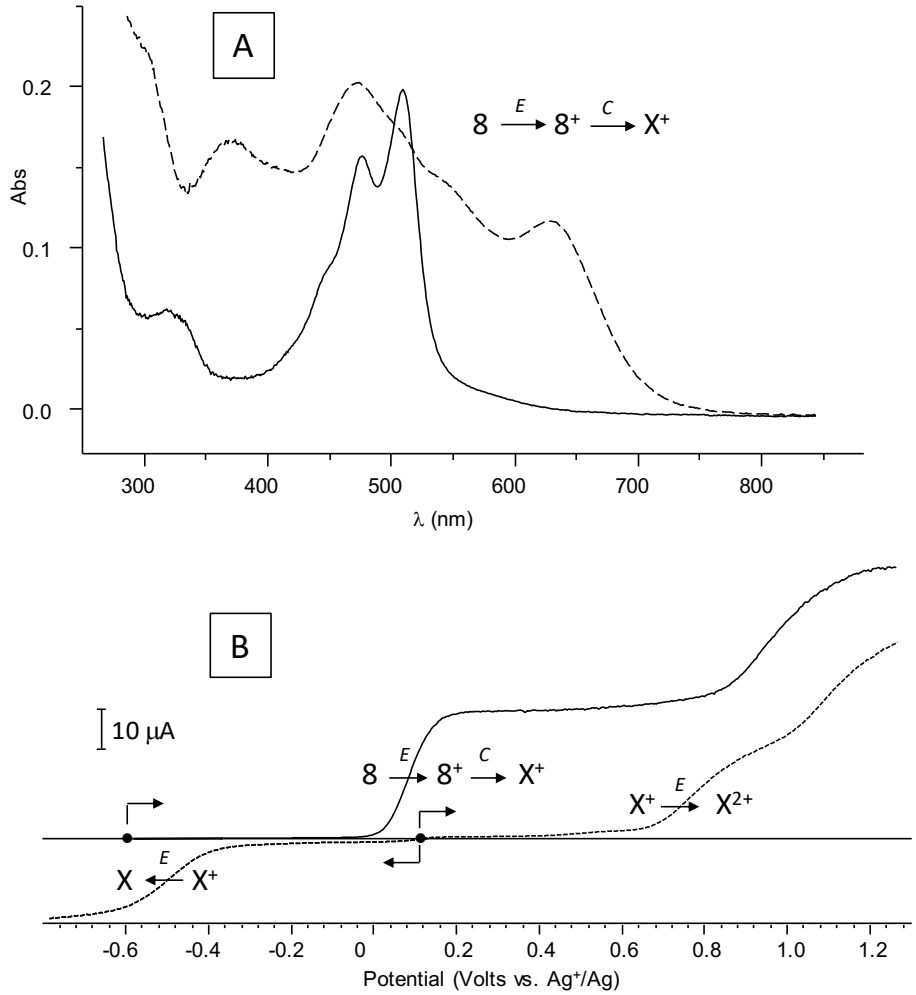

Figure 3 A) UV-Vis absorption spectra and B) voltammetric curves of **8** recorded at a rotating disk electrode (vitr. carb, Ø = 3 mm, v = 0.01 $V \cdot s^{-1}$, 550 rd/min) before (full line) and after (dashed line) exhaustive one electron oxidation of **7** (1.3 mM, dichloromethane, 0.1 M $TPAPF_6$, Pt working electrode, E_{app} = 0.35 V vs Ag^+/Ag).

It should also be mentioned that the workup process (washing, chromatography) implemented after electrolysis leads to significant changes in the electrochemistry of the product which are not yet fully understood. One explanation is that different oxidation/protonation states of **7** might be involves in the process.

X-ray diffraction analyses carried out on a single crystal of complex **7** revealed the presence of a single nickel ion found in a square planar NOON coordination environment and of a BF_4 anion balancing the monocationic charge of the complex (Fig. 3).

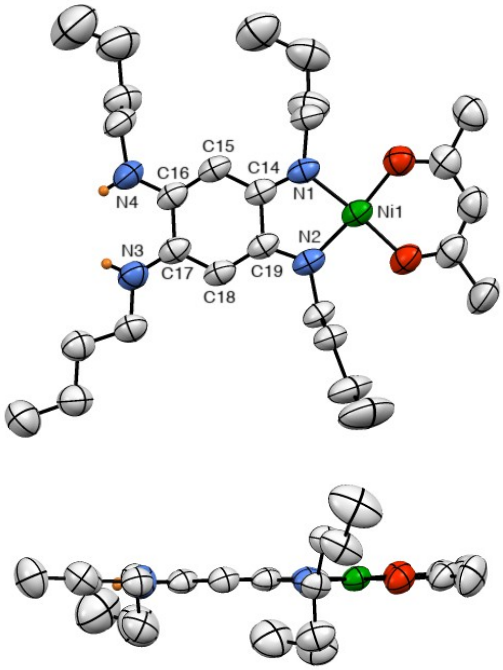

Figure 4 X-ray structure of **7**. Selected bond lengths (Å): N(4)-C(16) = 1.339(4), C(16)-C(15) = 1.371(5), C(15)-C(14) = 1.410(4), C(14)-N(1) = 1.306(4), N(3)-C(17) = 1.336(4), C(17)-C(18) = 1.382(4), C(18)-C(19) = 1.399(5), C(19)-N(2) = 1.323(4), C(14)-C(19) = 1.481(4), C(16)-C(17) = 1.493(4).

A close examination of the bond distances within the N(3)-C(17)-C(18)-C(19)-N(2) and N(4)-C(16)-C(15)-C(14)-N(1) moieties reveals an alternating succession of single and double bonds and the presence of two imine functions in *ortho* position [C(14)-N(1) and C(19)-N(2)], whereas C(16)-C(17) and C(14)-C(19) display typical single bonds distances of 1.493(4) and 1.481(4) Å, respectively. These data thus suggest a lack of conjugation between the two halves of the molecule and reveal that the coordination to Ni(II) leads to a *para*→*ortho* tautomerism of the ligand [6] providing a square planar NOON environment to the metal center. The ^{1}H NMR spectrum of **7** in $CDCl_3$ shows the presence of signals at 5.38 (I=1), 4.72 (I=2) and 4.57 (I=4) consistent with the acac C-H resonances, the central and external quinoidal C-H protons, respectively (see ESI section). Interestingly, comparative NMR studies carried out in CD_2Cl_2, DMSO-d_6 and pyridine-d_5 revealed that the coordination of DMSO or pyridine on the Ni(II) center leads to large up-field shifts of particular signals (down to the negative region of the spectra) attributed to a coordination-induced change in the spin state of the metal (from S= 0 to S = 1). This behavior will be further discussed in the following sections focusing on magnetic measurements.

3.2 UV-Vis Absorption Spectroscopy

The UV-Vis absorption spectrum of **7**, first recorded in DMSO at high concentration exhibits an intense band centered at 386 nm together with a weaker broad band at 490 nm (Fig. 4). Lowering the concentration was then found to result in the development of new absorption bands at 482 and 526 nm associated to the formation of the dinuclear complex **8**. These observations clearly demonstrate the high stability of **7** at large concentration in DMSO (coordinating solvent) and its ability to evolve spontaneously into the corresponding dinuclear species **8** at low concentration. Further studies carried out in a non-coordinating solvent like dichloromethane revealed the stability of **7** over all the entire investigated concentration range. These differences highlight the crucial role of the solvent and the kinetic lability of the N-Ni bonds in **7**. In other words, only the high spin (S= 1) form of **7** is able to rearrange into the dinuclear complex **8.** The UV-Vis absorption spectra shown in Fig. 6 reveal the drastic effect of the solvent on the spectroscopic signature of **7** (Fig. 6). The spectrum recorded in a non-coordinating solvent (CH_2Cl_2) exhibits an intense absorption band with vibronic peaks at 485 and 460 nm which gets blue shifted in coordinating solvents like pyridine or DMSO. The largest hypsochromic shift is as expected observed with the most coordinating solvent (pyridine), with a band centered at 345 nm, a shoulder at ca. 400 nm and a tiny absorption around 475 nm (Figure 5).

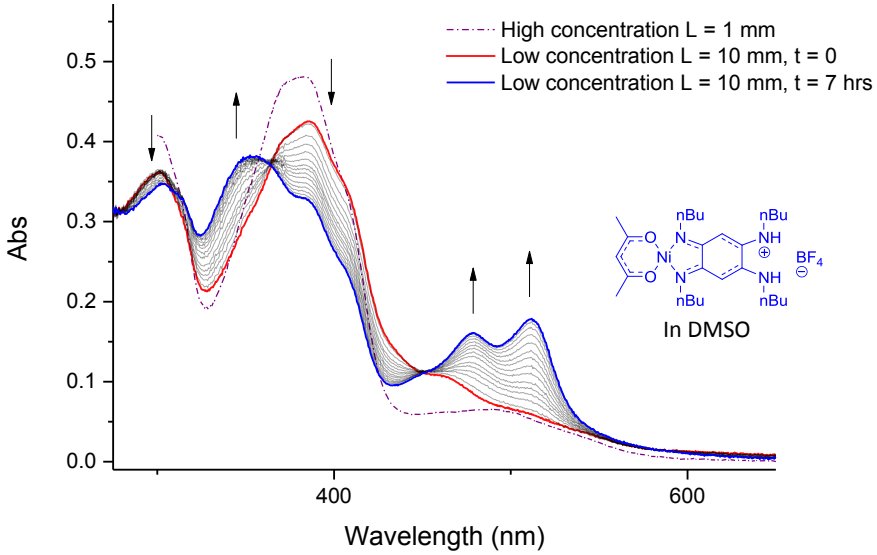

Figure 5 UV-Vis absorption spectra of **7** recorded in DMSO showing the influence of time and concentration (High concentration: [ ]~5.4E-04 M; Low concentration :[ ]~5.4E-05 M)

3.3 Theoretical Calculations

In order to gain more insights into the relationship between the electronic spectrum and the coordination sphere in **7**, theoretical calculations were performed using Time-Dependent Density Functional Theory (TD-DFT, see the SM for details). In our calculations, we considered both the

singlet and triplet cases in several environments: CH_2Cl_2, DMSO, and pyridine. For the former, no specific interaction between the molecule and the solvent is expected, and we used the well-known Polarizable Continuum Model (PCM) to describe environmental effects. For both DMSO and pyridine, we investigated the complexation of the nickel centre with one or two explicit solvent molecules, the full system being embedded in a PCM cavity.

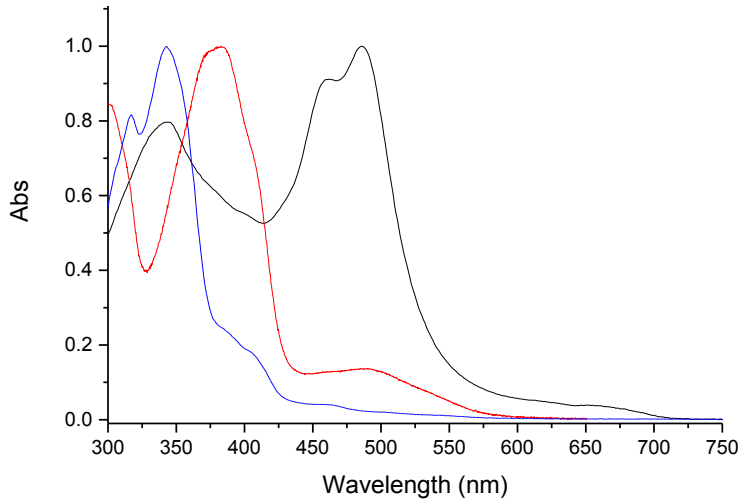

Figure 6 Electronic absorption spectra of **7** recorded in CH_2Cl_2 (black, L = 10 mm), DMSO (red, L = 1 mm) and pyridine (blue, L = 1 mm).

Selected optimal structures calculated for these structures are displayed in Fig 7 (see also SM). In DCM, the singlet form is clearly more stable by 24.9 kcal/mol, so that only that form should be present in solution. In DMSO, we compared the complexation by the oxygen and sulfur atoms for both singlet and triplet cases. For the singlet state, the S-bonding that is slightly favoured (1.6 kcal/mol with one explicit DMSO molecule, 0.3 kcal/mol with two explicit molecules), whereas, for the triplet spin state, the reverse is observed with a maximal stability for the O-Ni complexes that are more stable than the corresponding S-Ni structures by 0.3 kcal/mol (one explicit DMSO) and 10.6 kcal/mol (two explicit DMSO, Fig. 7). Irrespective of the consideration of one or two DMSO molecules, the most stable structure remains the triplet state, by 4.6 kcal/mol and by 12.6 kcal/mol with one and two DMSO molecules, respectively. In pyridine, the triplet state is also more stable by 8.0 kcal/mol and 13.3 kcal/mol with one and two pyridine molecules, respectively. In short, the triplet is clearly strongly favoured when solvent molecules coordinate the Ni atom. The strong interaction between pyridine molecules in the case of the triplet state is clear: it induces a pyramidal coordination (one pyridine molecule) or octahedral coordination (two pyridine molecules) around the nickel atom and significantly affects the distances of the coordination bonds (Table S1), whereas in the singlet case, a very limited impact is obtained.

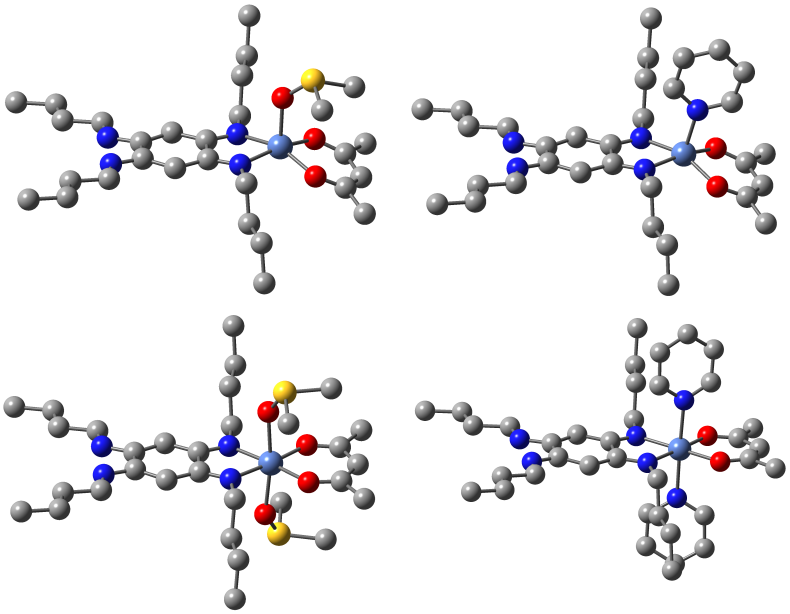

Figure 7 Optimized DFT structures of **7** for triplet systems considering DMSO (left) (with one or two explicit molecules, considering the most stable binding in each case) and pyridine (right) with one or two explicit molecules) as environment. Hydrogen atoms omitted for clarity.

As illustrated in Fig. 8 for the example of the pyridine solution, the spin density of the triplet excited-state is, as expected, mainly localized on the nickel atom with polarization of the coordinating atoms.

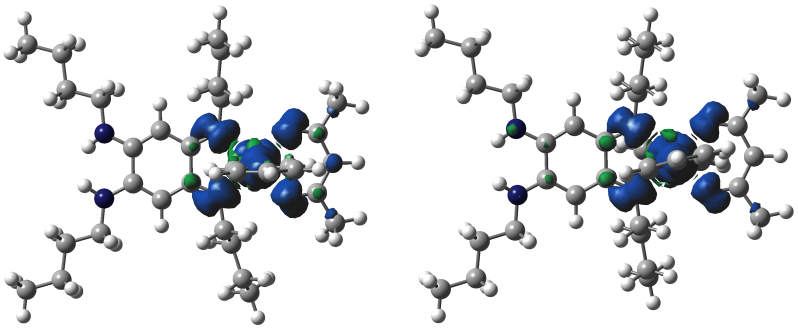

Figure 8 Spin density difference plots (threshold=0.001 au) for the triplet situation modelled with one (left) and two (right) explicit coordinating pyridine molecules.

For the singlet complex in CH_2Cl_2, TD-DFT foresees a series of very weak bands in the 580-650 nm domain, a first weak absorption at 549 nm (f=0.009) and a first strong absorption band at 430 nm (f=0.437) and a second at 358 nm (f=0.299). These two intense bands respectively involve to HOMO-1 to LUMO and HOMO-2 to LUMO excitations, and correspond to the experimentally intense ones observed at ca. 490 nm and ca. 386 nm, respectively, the blueshift of the theoretical results being a logical consequence of the lack of vibronic coupling in the modelling. We note that the LUMO is located on the phenyl ring and four vicinal nitrogen bonds, whereas the HOMO-1 and HOMO-2 are rather similar and encompass significant contributions on the acac (see the SM).

In contrast in the complex of **7** with one pyridine (triplet state), the first transition presenting a non-trifling oscillator strength (>0.025) is an excitation in the same spectral region as in the singlet case, but it is much less intense (428 nm, f=0.078), the second intense absorption band being located at almost the same position as in the singlet- CH_2Cl_2 case (363 nm, f=0.533). The situation is rather similar with two explicit pyridine molecules with very weak vertical absorptions at 487 nm (f=0.019) and 426 nm (f=0.027) and a much stronger one at 358 nm (f=0.571). This reasonably fits the experimental spectra of Fig. 6, with a large decrease of intensity of the long-wavelength band when going from CH_2Cl_2 to pyridine, but much smaller changes for the second band. With DMSO, the spectra computed for the most stable triplet state with one or two explicit solvent molecules are intermediate between the two previous cases. Indeed, the first band presenting an oscillator strength exceeding 0.025 can be found at 411 nm (f=0.086) or 394 nm (f=0.090) with one or two DMSO, respectively. The intense bands appear at 359 nm (f=0.489) and 349 nm (f=0.408) with one and two DMSO bonding the metallic centre, respectively. Again, there is an obvious qualitative match with the experiment displayed in Fi. 6.

3.4 Magnetism

Magnetic studies have been performed on liquid samples using sealed plastic straws containing complex **7** dissolved in pyridine (Fig. 9). The product of the magnetic susceptibility with temperature (χT) is as expected almost constant on the overall temperature range (240-300K) with a mean value of 1.04 emu K mol^{-1} which is in agreement with a Ni(II) ion (S=1, χT=1.0 for g=2) in a octahedral environment. The values calculated for all the investigated liquid samples is a little smaller than those generally obtained for HS Ni(II). This deviation is attributed to the existence of an equilibrium between the square planar and octahedral forms in pyridine.

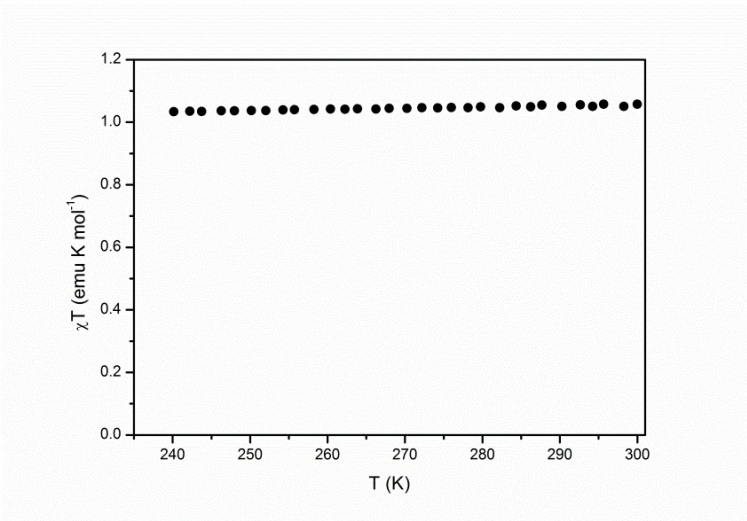

Figure 9. Temperature dependence of the product of the magnetic susceptibility (χT) with temperature (T) for complex **7** dissolved in pyridine.

4. CONCLUSION

In summary, we described three different syntheses of the first square-planar mononuclear nickel complex based on ligand **1** (**7**), in which the metal center is located in a tetradentate NOON environment. This complex is able to coordinate axial ligands with a tuneable strength (DMSO, pyridine) allowing the control the spin state and hence of the electronic properties. Despite the strength of the NOON ligand [13], a significant solvatochromism could be demonstrated through a combined experimental / theoretical study. This approach opens new perspectives in sensor applications because of the specific optical signature depending of the solvent.

ACKNOWLEDGEMENTS

This work was supported by the *Centre National de la Recherche Scientifique*, the *Ministère de la Recherche et des Nouvelles Technologies*. This works used computational resources of the IDRIS/CINES and of the CCIPL.

FOOTNOTES

Electronic supplementary information (ESI) available: theoretical calculations: methods and additional results for compound **7**.

REFERENCES

[1] (a) Brown ER. *The Quinonoid Compounds* (1988), John Wiley & Sons Inc, 2010;1231—1292.

(b) Hünig, S. Aromatic/quinoid systems: principles and applications. Pure Appl. Chem. 1990;62:395.

(c) Casado J, Ponce Ortiz R, Lopez Navarrete JT. Quinoidal oligothiophenes: new properties behind an unconventional electronic structure. Chem. Soc. Rev. 2012;41,5672.

(d) Lopez J., de la Cruz F., Alcaraz Y., Delgado F., Vazquez MA. Quinoid systems in chemistry and pharmacology. Med. Chem. Res. 2015;24:3599.

(e) Sarkar B, Schweinfurth D, Deibel N, Weisser F. Functional metal complexes based on bridging "imino"-quinonoidligands. Coord. Chem. Rev. 2015;293—294:250.

[2] Kimich C, Einwirkung A. Einwirkung aromatischer Amine auf Nitrosophenol und Nitrosodimethylanilin. *Ber. Dtsch.* Chem. Ges. 1875;8:1026.

[3] (a) Siri O, Braunstein P. First binuclear complex of an N,N',N'',N'''-tetraalkyl 2,5-diamino-1,4-benzoquinonediimine *Chem. Commun*. 2000;2223.

(b) Siri O, Braunstein P, Rohmer MM, Beńard M, Welter R. Novel "Potentially Antiaromatic", Acidichromic Quinonediimines with Tunable Delocalization of Their 6π-Electron Subunits. J. Am. Chem. Soc. 2003;125:13793.

(c) Khramov DM, Boydston AJ, Bielawski CW. Highly Efficient Synthesis and Solid-State Characterization of 1,2,4,5-Tetrakis(alkyl-and arylamino)benzenes and Cyclization to Their Respective Benzobis(imidazolium) Salts. Org. Lett. 2006;8:1831.

(d) Andeme Edzang J, Chen Z, Audi H, Canard G, Siri O. Transamination at the Crossroad of the One-Pot Synthesis of N-Substituted Quinonediimines and C-Substituted Benzobisimidazoles. Org. Lett., 2016;18:5340.

[4] Pascal S, Siri O. Benzoquinonediimine ligands: Synthesis, coordination chemistry and properties. Coord. Chem. Rev. 2017;350:178.

[5] Ohno K, Fujihara T, Nagasawa A. A. Formation of boron, nickel(II) and iridium(III) complexes with an azophenine derivative: Isomerization, delocalization and extension of the π-conjugated system on coordination. Polyhedron 2014;81:715.

[6] Frantz S, Rall J, Hartenbach I, Schleid T, Záliš S, Kaim W. Metal-Induced Tautomerization of p- to o-Quinone Compounds: Experimental Evidence from CuI and ReI Complexes of Azophenine and DFT Studies. Chem. Eur. J. 2004;10:149.

[7] Braunstein P, Demessence A, Siri O, Taquet J-p. Relocalisation of the pi system in benzoquinone-diimines induced by metal coordination. C. R. Chimie 2004;7:909.

[8] Rall J, Stange AF, Hübler K, Kaim W. Coordination-Induced 1,4→1,2-Quinonediimine Isomerization. Angew. Chem. Int. Ed. 1998;37:2681.

[9] Chen Z, Canard G, Jacquemin D, Bucher C, Giorgi M, Siri O. Hetero-Bimetallic Effect as a Route to AccessMultinuclear Complexes. Inorg. Chem. 2018;57:12536.

[10] (a) Masui H, Lever ABP. Correlations between the ligand electrochemical parameter, EL(L), and the Hammett substituent parameter, σ. Inorg. Chem. 1993;32:2199.

(b) Metcalfe RA, Vasconcellos LCG, Mirza H, Franco DW, Lever ABP. Synthesis and characterization of dinuclear complexes of 3,3',4,4'-tetraminobiphenyl with tetramminoruthenium and bis(bipyridine)-ruthenium residues and their two- and four-electron oxidized products including a ZINDO study of orbital mixing as a function of ligand oxidation state. J. Chem. Soc. Dalton Trans. 1999;2653.

[11] Ohtsu H., Tanaka K. Equilibrium of Low- and High-Spin States of Ni(II) Complexes Controlled by the Donor Ability of the Bidentate Ligands. Inorg. Chem. 2004;43:3024.

[12] Fukuda Y, Akutagawa Y, Ihara Y, Sone K. Solvatochromism of Nickel(II) Mixed Chelates Containing Acetylacetonate and Some Cyclic Diamines. Synth. React. Inorg. Met. Org. Chem. 1991;21: 313.

[13] Gonciarz A, Zuber M, Zwozdziak J. Spectrochemical Properties and Solvatochromism of Tetradentate Schiff Base Complex with Nickel: Calculations and Experiments. Chemistry Open 2018;7:677.